Journal of Sound and Vibration (1999) **224**(1), 1–16
Article No. jsvi.1997.1070, available online at http://www.idealibrary.com on IDEAL ®

MODE SHAPES DURING ASYNCHRONOUS MOTION AND NON-PROPORTIONALITY INDICES

A. Bhaskar†

Department of Aerospace Engineering, *Indian Institute of Science*, *Bangalore* 560 012, *India*

(*Received* 29 *August* 1995; *and in final form* 26 *March* 1997)

When synchronous motion does not exist, it is not possible to draw the classical mode shapes. In this paper, a representative shape of motion during free vibration of a non-classically damped system is sought. It is noted that this shape provides an optimal representation of free motion. Interpretations of the optimality thus introduced are presented. Their connection with non-proportionality of damping and of gyroscopy is brought out. In the spirit of the optimality presented in this paper, two indices of non-proportionality are defined. Properties of these indices are discussed. Comparison with other indices of non-proportionality available in the literature is presented. Illustrative examples are given.

1. INTRODUCTION

A dynamical system, in general, possesses complex eigenvectors. The free vibratory motion is then asynchronous. There are, however, three notable exceptions to this general case: (i) when the system is undamped (see references [1, 2] for example), (ii) when the system is damped, but damping is classical [3–5], and (iii) when the system possesses gyroscopy but the matrices involved satisfy conditions very similar to those of (ii) (Liu and Wilson [6]). In all these cases, synchronous motion is possible only for certain combinations of initial conditions. Very few authors draw mode shapes for damped systems, since classical normal modes do not exist for a general case of damping (the corresponding eigenvectors are complex). Usefulness of complex eigenvectors for a direct interpretation is limited because the ratio of the components of the vector of generalised displacements changes during motion. In this paper, a graphical representation of a complex mode is sought.

Luo [7] presents a graphical method of depicting free vibration of a damped mode by using a number of spirals, where each spiral represents motion of a

† Present affiliation: Department of Aeronautaics and Astronautics, University of Southampton, Southampton SO17 1BJ, U.K.

0022–460X/99/260001 + 16 $30.00/0

co-ordinate on the complex plane. Although this is a complete representation, in the opinion of the present author, these spirals elucidate little about the deformed "shape" of the system involved during free vibration. There is thus limited practical value of the diagrams presented in reference [7]. A second treatment, presented by Newland [2, 8], utilizes a collection of successive configurations during motion at various instants of time over one period. This method is intuitively more appealing, since the purpose of examining a mode shape is often to learn about the relative magnitudes of motion of various generalised co-ordinates. However, it requires calculation of many such "snap-shots" (ideally infinitely many, to preserve complete information) in order to describe motion of a given damped mode. The present work is inspired by this approach; the departure is an attempt to arrive at a single diagram which can be used as a representative mode shape when an eigenvector is complex. Needless to say, there can be no instant of time during motion at which the motion can be regarded as truly synchronous. Therefore, loss of information is inevitable if one is to draw a single deformed configuration as a representative of a complex mode. The author's concern here is to look for an instant of time for which different co-ordinates can be regarded as executing motion which is as close to being in-phase or out-of-phase motion as possible.

2. THE EIGENVALUE PROBLEM FOR GENERAL DYNAMICAL SYSTEMS

The equations of motion for a damped gyroscopic system in the absence of circulatory forces and external forcing are given by (see for example [1])

$$\mathbf{M}\ddot{\mathbf{x}} + (\mathbf{C} + \mathbf{G})\dot{\mathbf{x}} + \mathbf{K}\mathbf{x} = \mathbf{0}. \tag{1}$$

Here $\mathbf{M}$ stands for the inertia matrix, $\mathbf{C}$ for the damping matrix, $\mathbf{G}$ for the gyroscopic matrix, $\mathbf{K}$ for the stiffness matrix, and $\mathbf{x}$ for the vector of generalised co-ordinates. The total number of degrees of freedom is n. Matrices $\mathbf{M}$ and $\mathbf{C}$ are assumed to be positive definite while the stiffness matrix $\mathbf{K}$ is assumed to be positive semi-definite. The gyroscopic matrix $\mathbf{G}$ is skew-symmetric. Defining the state vector $\mathbf{z}$ as $\mathbf{z} = [\dot{\mathbf{x}}^{\mathrm{T}}|\mathbf{x}^{\mathrm{T}}]^{\mathrm{T}}$, equation (1) can be recast as

$$\dot{\mathbf{z}} = \mathbf{A}\mathbf{z}, \tag{2}$$

where

$$\mathbf{A} = \begin{bmatrix} -\mathbf{M}^{-1}(\mathbf{G} + \mathbf{C}) & -\mathbf{M}^{-1}\mathbf{K} \\ \mathbf{I} & \mathbf{0} \end{bmatrix}.$$

The corresponding eigenvalue problem is

$$\mathbf{A}\mathbf{z} = \lambda\mathbf{z}, \tag{3}$$

where $\mathbf{z}$ represents the $2n$-dimensional eigenvector and λ the eigenvalue. From here onwards, a vector of the kind $\mathbf{z}$ will be interpreted as the state-vector (as in equation (2)) or the eigenvector in the state-space (as in equation (3)) depending on the context. Similarly, $\mathbf{x}$ represents the vector of generalised co-ordinates (as

in equation (1)) as well as the last n elements of the eigenvector $\mathbf{z}$. Since $\mathbf{A}$ is a real but an asymmetric matrix, its eigenvalues (and eigenvectors) are, in general, complex. The real and imaginery parts of the rth eigenvalue can be separated as

$$\lambda_r = -\alpha_r + \mathrm{j}\omega_r, \tag{4}$$

where α_r is the decay rate of the mode in question, ω_r is the corresponding damped natural frequency (see reference [2]) and $\mathrm{j} = \sqrt{-1}$. The case of real eigenvalues is omitted from the discussion, since they correspond to non-oscillatory (overdamped) motion and are essentially synchronous.

2.1. GRAPHICAL REPRESENTATION OF COMPLEX EIGENVECTORS

Methods based on the trajectories of the co-ordinates in the complex plane and those based on the snap-shots of free vibratory motion were described in section 1. A few other possible alternatives of representing a complex eigenvector graphically are discussed next using an example.

Since the ratio of generalised displacements corresponding to different co-ordinates remains the same during synchronous motion, one can think of nodes in a classical normal mode. In case of a system in which classical modes do not exist, there is no such stationary point and the point having zero displacement fluctuates during motion. Consider an eigenvector $\mathbf{z} = [\lambda\mathbf{x}^{\mathrm{T}}|\mathbf{x}^{\mathrm{T}}]^{\mathrm{T}}$ of the eigenvalue problem (3) where $\mathbf{x} = [1 - 0{\cdot}5\mathrm{j},\ -0{\cdot}75 + 0{\cdot}5\mathrm{j},\ 1 - 0{\cdot}5\mathrm{j}]^{\mathrm{T}}$ and $\lambda = -0{\cdot}2 + \mathrm{j}$. A possible representation of the eigenvector (assuming its origin is a three-degree-of-freedom system constrained at the two ends) is shown in Figure 1. There are two "mode shapes" in this case: the real mode and the imaginary mode (Figure 1(a)). Another alternative is to plot magnitudes and phases of the co-ordinates involved. Plotting only the real part or only the magnitude will be an incomplete representation.

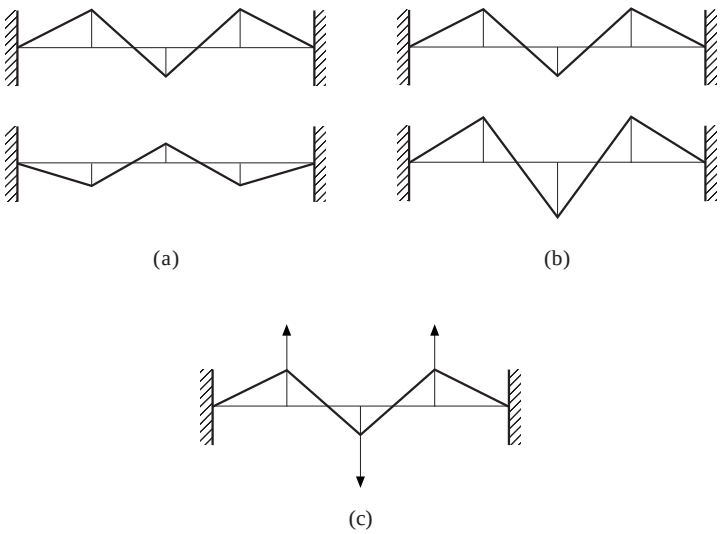

Figure 1. Three representations of complex modes by means of: (a) real and imaginary parts, (b) displacements and velocities and (c) displacements and velocities superposed on a single diagram.

Recalling that a general dynamical system can be decoupled in the state space, it can be inferred that a damped mode demands a plot in the state-space rather than that in the configuration space. Hence a plot which shows both displacements as well as velocities carries complete information. This is chosen to be represented by plotting displacements $\mathscr{R}(x)$ against the co-ordinates and displaying it along with the corresponding velocities $\mathscr{R}(\lambda\mathbf{x})$ required in order to observe motion in a damped mode. Here $\mathscr{R}(\cdot)$ represents the real part of $(\cdot)$. Figure 1(b) is such a representation. Yet another alternative is to plot displacements and superpose on the same figure the corresponding velocities by using arrows (see Figure 1(c)). Had the system been classically damped, the length of the arrows would then have been proportional to the displacements at the corresponding co-ordinates and the information carried by the velocity arrows would have been redundant. The phase information between various co-ordinates, which is different for different co-ordinates, is possessed by the velocities (i.e., those with $\mathscr{R}(\lambda\mathbf{x})$). To the best of the author's knowledge, this simple graphical representation of a complex mode which contains complete information by combining displacements and velocities during motion is unavailable in the published literature. A more involved method of obtaining an optimal mode shape for a non-classically damped mode is discussed in the next section.

3. THE OPTIMAL MODE SHAPE

In this paper, an instant of time during asynchronous motion is identified such that the corresponding state can be considered to be as close to being synchronous as possible. Before proceeding on to the idea of synchroneity the following must be made clear: since all the co-ordinates of a system execute motion with the same frequency, namely the damped natural frequency, the phase difference between any two co-ordinates remains constant for all instants of time. From this point of view, when synchroneity is measured by the phase between two sinusoids, every time instant must be treated on equal footing. Therefore, so far as relative phase between various co-ordinates is the only consideration, configuration at every point of time must be regarded as equally synchronous or asynchronous.

Let one take another look at this situation. One first asks the following question: ''Is there a configuration which deviates least from all other configurations during the course of motion?''. One can find such a configuration in more than one way depending on the definition of ''least deviation''. This configuration can then be regarded as the representative snap-shot and could then be used as the ''optimal mode shape''. An elegant answer is provided by approaching the problem geometrically.

Consider the phasor diagram of Figure 2. Each element of a typical complex eigenvector is plotted using an arrow on this diagram. The deformed shape during motion is obtained by plotting the real part for each arrow against the generalised co-ordinates. The whole diagram rotates with an angular velocity equal to the imaginary part of the eigenvalue corresponding to this eigenvector. Let the kth eigenvector be $\mathbf{z}_k$. The elements of this eigenvector are given by $[\lambda_k\mathbf{x}_k^{\mathrm{T}}|\mathbf{x}_k^{\mathrm{T}}]^{\mathrm{T}}$, where λ_k is the kth eigenvalue of the eigenvalue problem (3). If the motion were

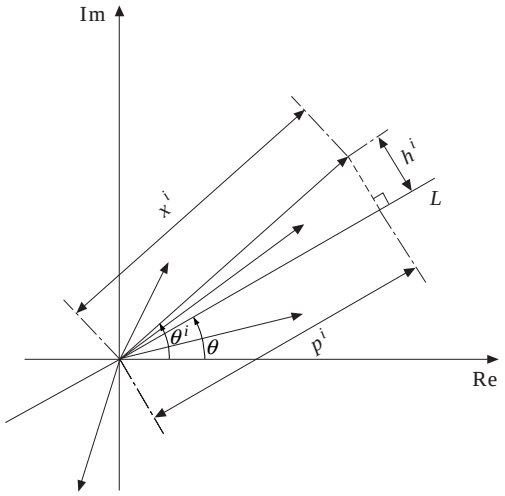

Figure 2. Representation of an eigenvector on the complex plane. Projections of the ith component x^i along and orthogonal to an arbitrary line L are denoted by p^i and h^i respectively.

synchronous, all the phasors would collapse to a line. If a mode is "nearly synchronous" then the phasors are expected to be spread in a small sector on the complex plane (which is a perturbation on synchronous motion) and the change in deformed configuration during motion is expected to be small. This suggests the following geometrical question: "Is there a line through the origin on Figure 2 which can be regarded as closest (in a given sense) to all the phasors?" Projections on this mean line could then be used to reconstruct the corresponding configuration. A reasonable solution is the line obtained by minimising the sum of squares of orthogonal components (shown for the ith phasor by h^i). This is equivalent to maximising the sum of squares of projections. The projections along L are denoted by p^i. Consider the vector of the last n components of the kth eigenvector denoted by $\mathbf{x}_k$. In what follows, the subscript has been dropped for convenience. Components of this vector will be denoted subsequently by an index appearing in the superscript. The sum of squares of projections along and orthogonal to an arbitrary line L through the origin (Figure 2) is given by

$$\sum_{i=1}^{n} (p^i)^2 + \sum_{i=1}^{n} (h^i)^2 = \mathbf{x}^{\mathrm{H}}\mathbf{x},$$

which is a constant irrespective of the choice of the line L. Here $(\cdot)^{\mathrm{H}}$ represents the conjugate transpose of $(\cdot)$ and where $\mathbf{x}$ is the vector of the last n elements of the eigenvector in question. The line through the origin on the complex plane which maximises the sum of the squares of the projection onto it, will be referred to as L_{opt}.

It is now claimed that the mode shape obtained by projecting phasors onto L_{opt} provides the optimal mode shape. The basis is that the motion is synchronous (and correspondingly, a classical normal mode exists) if the phasors are aligned. Mode shapes obtained in this way can be regarded as the optimally synchronous

approximation to an asynchronous motion since the component of a phasor orthogonal to the line L_{opt} can be considered as the asynchronous component of the phasor in question. The configurations at successive stages of motion can be obtained by taking the real part of these phasors while they rotate. Nodes can be observed in the animations obtained in this way, since all the co-ordinates are necessarily in-phase or out-of-phase. The configuration obtained by plotting the projections (against the generalised co-ordinates) onto L_{opt} denotes a representative (or average) configuration of motion of the damped natural mode in question. This configuration is observed twice in one cycle.

Since scaling by a complex scalar is equivalent to scaling the magnitude of phasors as well as rotating them, the optimal mode shapes can be obtained by suitably scaling the original phasors and plotting their real parts. This gives us a further interpretation of an optimally synchronous mode: it is a mode shape obtained by appropriately scaling the eigenvectors (using a complex scaling factor) such that the sum of the squares of the imaginary parts is minimal.

3.1. MAXIMISATION OF THE SUM OF THE SQUARES OF PROJECTIONS

The projection of the ith component of the phasor $\mathbf{x}$ along the ray $\exp(j\theta)$ is given by

$$p^i = |x^i| \cos(\theta^i - \theta) \tag{5}$$

and the component orthogonal to it is given by

$$h^i = e^i = |x^i| \sin(\theta^i - \theta), \tag{6}$$

where θ^i is the phase of the phasor x^i and θ is phase of the ray. Hence the total squared projection P and the total squared "error" E are given by

$$P = \sum_{i=1}^{n} (p^i)^2 \qquad \text{and} \qquad E = \sum_{i=1}^{n} (e^i)^2 = \sum_{i=1}^{n} (h^i)^2. \tag{7}$$

Applying the condition that $\partial P/\partial\theta = 0$ for an extremum of P, one obtains

$$\tan(2\theta) = S/C, \tag{8}$$

where the numerator and the denominator are given by

$$S = \sum_{i=1}^{n} |x^i|^2 \sin 2\theta^i \qquad \text{and} \qquad C = \sum_{i=1}^{n} |x^i|^2 \cos 2\theta^i. \tag{9}$$

Equation (8) has four general solutions for θ in the range $0 \leqslant \theta \leqslant 2\pi$ as $\theta = \overline{\theta}$, $\overline{\theta} + \pi$, $\overline{\theta} \pm \pi/2$, where $\overline{\theta} = (1/2)\tan^{-1}(S/C)$. Note that the first and the second; and the third and the fourth solutions represent two lines through the origin which are perpendicular to each other and they correspond to an extremum of P. The condition for a maximum is $\partial^2 P/\partial\theta^2 < 0$ which can be simplified to

$$\sum_{i=1}^{n} |x^i|^2 \cos 2(\theta^i - \theta) > 0. \tag{10}$$

It can be checked that out of the four solutions for θ mentioned earlier, there are two which satisfy the condition for a maximum and two for a minimum. Therefore, amongst all the successive stages of free damped motion, there exists a configuration which can be considered as the one which resembles the overall motion least (in the least square sense defined earlier). We also realise that the most synchronous and the least synchronous motions are separated by a phase $\pi/2$.

4. EXAMPLES AND DISCUSSIONS

The following examples illustrate the observations made in the earlier sections.

Example 1. This numerical example is based on a seven degree-of-freedom lumped parameter model of a chimney on a resilient foundation and is discussed at length by Newland [2]. The model consists of seven rigid bars of length l each having mass equal to m concentrated at the centre of each of the bars and interconnected by torsional springs of stiffness k at the joints, except at the base where the torsional stiffness is K. A sketch can be found in reference [2] or [8]. The mass matrix is given by

$$\mathbf{M} = m_1 \begin{bmatrix} 0 & 0 & 0 & 0 & 0 & 1 & 1 \\ 0 & 0 & 0 & 0 & 1 & 4 & 3 \\ 0 & 0 & 0 & 1 & 4 & 8 & 5 \\ 0 & 0 & 1 & 4 & 8 & 12 & 7 \\ 0 & 1 & 4 & 8 & 12 & 16 & 9 \\ 1 & 4 & 8 & 12 & 16 & 20 & 11 \\ 4 & 8 & 12 & 16 & 20 & 24 & 13 \end{bmatrix}$$

and the stiffness matrix is given by [2]

$$\mathbf{K} = k_1 \begin{bmatrix} 0 & 0 & 0 & 0 & \kappa & (-2\kappa+1) & (\kappa-1) \\ 0 & 0 & 0 & \kappa & (-2\kappa+3) & (\kappa-2) & -1 \\ 0 & 0 & \kappa & (-2\kappa+5) & (\kappa-2) & -2 & -1 \\ 0 & \kappa & (-2\kappa+7) & (\kappa-2) & -2 & -2 & -1 \\ \kappa & (-2\kappa+9) & (\kappa-2) & -2 & -2 & -2 & -1 \\ (-2\kappa+11) & (\kappa-2) & -2 & -2 & -2 & -2 & -1 \\ \kappa_1-2 & -2 & -2 & -2 & -2 & -2 & -1 \end{bmatrix},$$

where $m_1 = ml/4$ and $k_1 = mg/2$, $\kappa = 2k/mgl$, $\kappa_1 = 2K/mgl$; and where g is the acceleration due to gravity. Note that both of these matrices are asymmetric but they can be symmetrised after rearranging the rows and the columns. Numerical values for this example are taken from Newland [2] as: $l = 6$ m, $m = 3 \times 10^3$ kg, $k = K = 10^9$ Nm/rad and $c = 5{\cdot}85 \times 10^7$ Nms/rad. Entries on the damping $\mathbf{C}$

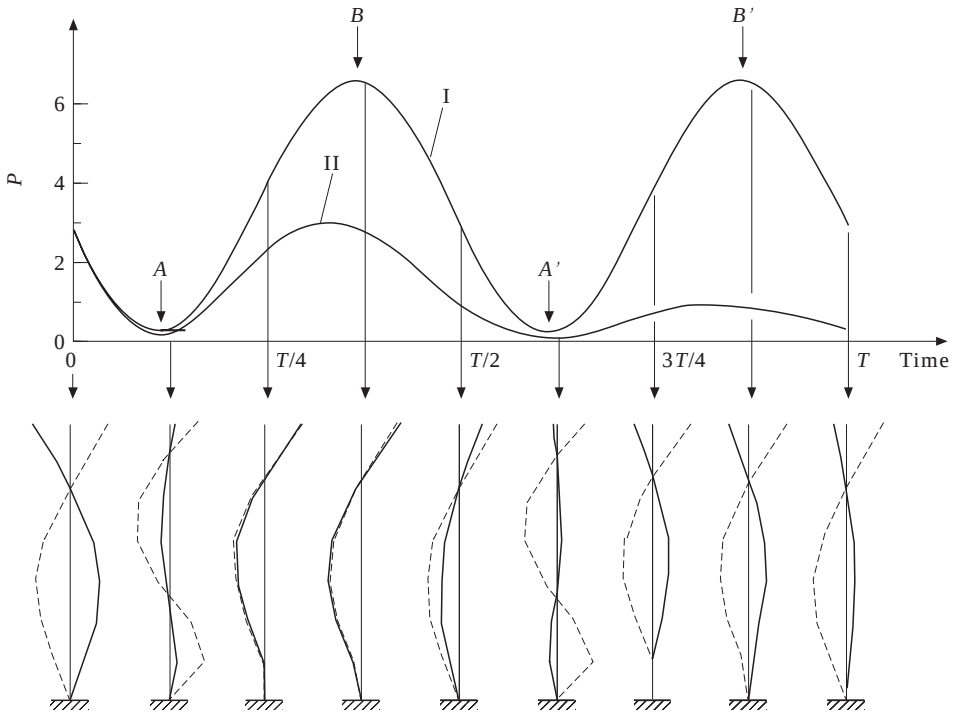

Figure 3. Successive stages of motion plotted at an interval of $T/8$ (bottom portion of the figure); T being the period of free vibration and graphs of the total squared projection (top portion of the figure).

matrix are given by $C_{ij} = 0$ for all i, j except for $C_{71} = c/l$, c being the dashpot constant of the foundation.

Successive shapes of damped free motion of the second damped mode are shown in Figure 3 (the set of sketches at the bottom of the figure) drawn at a stroboscopic time interval of $T/8$ where T is the period. In each case, the solid line represents the configuration observed during damped motion with increasingly diminishing amplitude of motion. Corresponding dotted lines are scaled such that the maximum value of displacement in each figure is $+1$. This way the solid lines describe the actual configurations during damped motion whereas the dotted lines represent the corresponding (different!) "shapes" during the motion. It may be recalled that the shape of motion stays unchanged during a synchronous motion. In the same figure, the plot of the sum of squares of projections of all the phasors corresponding to the second damped mode is shown as a function of time (see the continuous graph drawn above the snap-shots of deformation shapes). Peaks of the curve marked I correspond to the time instant at which the "optimal mode shape" is observed during motion. In a similar manner, troughs relate to the "least synchronous" modes discussed previously. The time instants of peaks (labelled B and B′) and troughs (labelled A and A′) have been indicated using vertical arrows in each case. The second curve on the same graph marked II is calculated after accounting for the diminishing length of the phasors due to damping. Points on curve I have been calculated by rotating the original phasors without letting their lengths change. The peaks and the troughs of curve I and curve II do not, in

general, occur at the same instant of time. This analysis which seeks the optimal deformed configuration is based on curve I since this curve has peaks and troughs occurring at fixed time intervals.

Shapes drawn using the dotted lines in Figure 3 repeat with a period of $T/2$ and not T and they represent out-of-phase motion. The frequency of curve I is double the damped natural frequency. The reason is that the frequency of the sum of *squares* of projection on the real line is double that of the rate of rotation of the phasors. Therefore, referring to Figure 3, the dotted configuration of the first and the fifth positions are the same, those of the second and the sixth positions are the same and so on. This mens that while drawing successive positions during motion, it is adequate to draw snap-shots of motion up to only half the period of damped oscillation. This fact does not seem to have been recognised elsewhere.

The calculated optimal mode shapes are presented in Figure 4(a) (left to right as the damped natural frequency increases). The corresponding least synchronous modes are shown in Figure 4(b). To examine if there is any resemblance of the optimal damped modes with the undamped modes, damping has been set to zero and the corresponding undamped modes have been plotted in Figure 4(c). Comparing Figures 4(a) and 4(c), it is observed that the optimal modes perform fairly satisfactorily in representing the shape of motion in situations where the synchronous shapes do not exist.

In this example, the number of undamped natural frequencies (and hence the corresponding number of natural modes) is seven whereas there are only six damped oscillatory modes. The reason is that the number of complex conjugate pairs of eigenvalues for the damped eigenvalue problem is not the same as the number of undamped natural frequencies. Therefore, it is not possible to establish a one to one correspondence between the undamped modes and the damped ones in this case because when damping is included, non-oscillatory (or overdamped) modes result. Due to the non-oscillatory character of a damped mode, the phasor

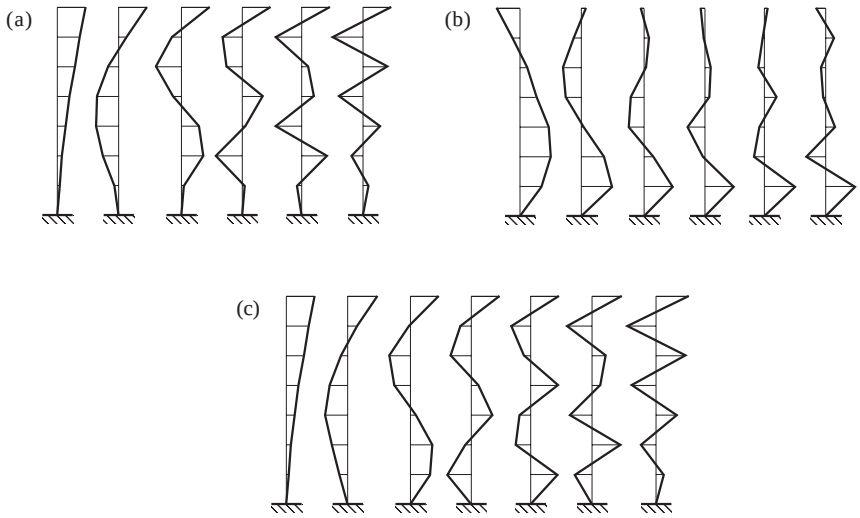

Figure 4. Mode shapes for the chimney problem of Example 1: (a) optimally synchronous oscillatory modes for the damped modes, (b) least synchronous damped oscillatory modes and (c) normal modes for the corresponding undamped problems.

representation has no meaning. Since overdamped modes are associated with real eigenvectors, they can be treated as synchronous. Therefore, the overdamped modes have been omitted from the calculations. Comparing Figures 4(a) and 4(c), one can observe that the first and second optimal modes of Figure 4(a) resemble the first and the second modes of Figure 4(c) whereas the fifth and the sixth optimal modes of Figure 4(a) resemble the sixth and the seventh modes of Figure 4(c). The case of the remaining intermediate modes is less clear. The third and the fourth optimal modes represent the dominant motions corresponding approximately to the undamped motions in the third, the fourth and the fifth undamped natural modes. Returning to the deformed shapes of Figure 4(b), one notices that for *all* the modes, the co-ordinate of the lowest unconstrained point has a large amplitude, a fact not confirmed by the sketches of undamped modes. This is expected since the shapes drawn in Figure 4(b) are supposed to be the least dominant ones amongst those that are realised in every cycle during motion, and hence not representative.

5. INDICES OF NON-PROPORTIONALITY

When damping is non-classical, various authors have formulated indices in order to quantify the extent of non-proportionality. Prater and Singh [9] proposed indices (a) based on the area of the modal polygons, (b) in terms of modal phase differences, (c) in terms of relative magnitude of coupling terms in the normal co-ordinate damping matrix and finally (d) those based on response. Subsequently, Nair and Singh [10] proposed a further two indices of non-proportionality on the basis of constraint matrices and the Nyquist plot. Bellos and Inman [11] defined a non-proportionality index in terms of the driving frequency and elements of the modal damping matrix. A non-proportionality index based on the error that is introduced by ignoring coupling terms of the modal damping matrix was proposed by Bhaskar [12, 13]. With the exception of [9] most of these indices work directly with the system matrices and not the eigenvectors. Non-proportionality is also closely related to the concept of modal coupling. In this reagard, two very similar papers by Park *et al*. [14, 15] are worth mentioning.

From the discussions in the previous sections it is clear that the eigenvectors of a classically damped system when represented on the complex plane collapse to a straight line passing through the origin. Guided by this, Prater and Singh [9] developed an index of non-proportionality based on the areas of ''modal polygons''. Before going into the details, it is proper to mention two things: firstly, there can be no unique definition of the index of non-proportionality. Secondly, all the indices must possess certain desired behaviour in the limiting cases of non-proportionality.

Prater and Singh [9] obtained a closed polygon on the complex plane by joining vertices of the tips of the vectors of the individual components of an eigenvector. The area of this polygon (called the modal polygon) when normalised with respect to the maximum modal area (area of a regular polygon) is defined in reference [9] as a non-proportionality index. It was rightly recognised there that if one or more displacement(s) is(are) out-of-phase, then the index proposed there will be an

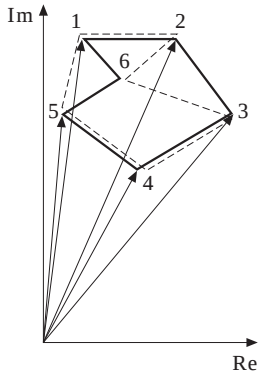

Figure 5. An example of an eigenvector plotted on the complex plane which shows that the definition of a "modal polygon" is ambiguous.

inconsistent index, since the modal polygon would have a very large area despite the system being only slightly non-proportional. A remedy was proposed to overcome this problem by rotating each of the "out-of-phase" displacements through π and then reconstructing the modal polygon [9]. This solution is not always satisfactory. There are other problems too with this index which are discussed next:

(1) The definition of modal polygons presented in reference [9] is not unique. Consider a hypothetical situation in Figure 5 which represents an eigenvector of a six-degree-of-freedom system. In this case, it is not clear if one should construct a modal polygon by joining points 1–2–3–4–5–6–1, in that order, (the solid line) or by joining points 1–2–6–3–4–5–1 (the dotted line) or by 1–2–3–6–4–5–1 etc. The other possibility is to join the points in the order in which the generalised co-ordinates appear (the problem is that the lines cross each other in certain situations). Yet another possibility is to take the convex hull of all the points to define modal polygons. In each case, the non-proportionality index as defined in [9] has a different value! It is clear that uniqueness of the definition of the index based on modal polygons presented in [9] is limited to convex polygons only (a convex polygon is one which contains all the straight lines obtained by joining any two points in its interior or on its boundary).

(2) Orientation of a modal polygon does not affect the value of the non-proportionality index as defined in [9]. This is not desirable because a thin and long convex polygon is associated with an approximately proportionally damped system if the longer dimensions of this polygon orient themselves close to a radial direction. To illustrate this point, consider two triangles ABC and A′B′C′ in Figure 6. The two triangles are congruent and thus they would have the same value of non-proportionality index based on modal polygons of [9]. However, one notes that co-ordinates 1 and 2 (corresponding to points A and B respectively) are, in fact, synchronous and the phase difference with the third co-ordinate is small. In contrast, the primed system A′B′C′ exhibits strong non-proportionality which the area of the modal polygon fails to capture. As an extreme case, if we changed the system parameters such that A and A′ fall on BC and B′C′ respectively, both polygons would have zero area and hence would

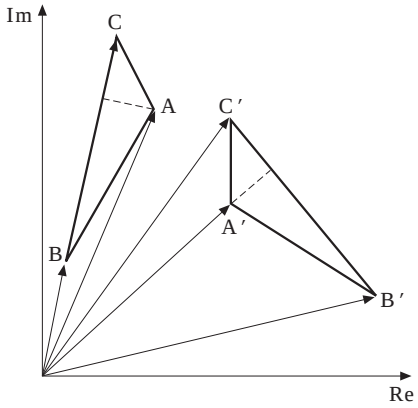

Figure 6. An example of two eigenvectors with distinctly different non-proportionality but having identical area of the respective modal polygons.

predict absence of non-proportionality. In the case of system ABC, it is true (since BC is a radial line), but in the case of B′C′ it is not. This is most undesirable. The basic problem with this index lies in the fact that areas of the modal polygons do not always represent the phase information correctly.

(3) A two-degree-of-freedom system always has a "modal polygon" as a straight line (and hence zero area thereof). A non-proportionality index based on area of modal polygons then always predicts classical damping for a two-degree-of-freedom system. This prediction is correct when the line representing the modal polygon is radial but is incorrect when it is not. In the author's opinion this is a serious inconsistency in the definition of a non-proportionality index.

(4) Modal polygons having out-of-phase (or nominally out-of-phase) displacement phasors exhibit unreasonably large value of the area of the modal polygons. This difficulty was tackled in reference [9] by rotating each of the out-of-phase phasors through π, such that the modal polygons are confined to the first and the fourth quadrants. This may lead to discontinuity of the non-proportionality index with respect to changes in the system parameters. To demonstrate this, consider a situation in which a given component of an eigenvector is close to having negative imaginary such that the arrow corresponding to this component points approximately in the direction $-j\infty$ when plotted on the complex plane. It can be seen that minor variations in system parameters which may bring about a change in sign of the small real part of this complex component of the eigenvector in question, will cause a jump in the value of the area of the modal polygon, if the prescription of rotating out-of-phase or nominally out-of-phase vectors through an angle π is followed.

5.1. A NEW INDEX OF NON-PROPORTIONALITY

Guided by the shortcomings of the non-proportionality index based on modal polygons, a non-proportionality index is defined in the spirit of the present discussions of sections 3 and 4 as

$$\eta = \sqrt{E/P}, \tag{11}$$

where the quantities E and P are defined by equation (7). The non-dimensional quantity η can be used as a measure of non-classicality and/or gyroscopic coupling. This index can be interpreted as the ratio of the root mean square value of the "error" and the root mean square value of the "model". Error relates to the non-classical effects whereas model pertains to proportional damping. Hence η measures deviations from the proportional damping model.

Example 2. Sometimes modes may appear to be fairly complex but in fact they can be rendered to a mode close to a real one by scaling. An extreme case of this is the computed eigenvector for a classically damped system which may show a significant phase but this phase stays the same for all the co-ordinates. Therefore, it is not the absolute phase, but the relative spread of the phases for various co-ordinates which determines how asynchronous a mode is. To illustrate this in the light of the previous discussions, consider a three-degree-of-freedom system whose governing equations of motion, are given by

$$\begin{bmatrix} m_1 & 0 & 0 \\ 0 & m_2 & 0 \\ 0 & 0 & m_3 \end{bmatrix} \begin{Bmatrix} \ddot{x}_1 \\ \ddot{x}_2 \\ \ddot{x}_3 \end{Bmatrix} + \begin{bmatrix} (c_1 + c_2) & -c_2 & 0 \\ -c_2 & (c_2 + c_3) & -c_3 \\ 0 & -c_3 & c_3 \end{bmatrix} \begin{Bmatrix} \dot{x}_1 \\ \dot{x}_2 \\ \dot{x}_3 \end{Bmatrix}$$

$$+ \begin{bmatrix} (k_1 + k_2) & -k_2 & 0 \\ -k_2 & (k_2 + k_3) & -k_3 \\ 0 & -k_3 & k_3 \end{bmatrix} \begin{Bmatrix} x_1 \\ x_2 \\ x_3 \end{Bmatrix} = \begin{Bmatrix} 0 \\ 0 \\ 0 \end{Bmatrix}.$$

For the data $m_1 = m_2 = m_3 = 1$, $k_1 = 1$, $k_2 = 4$, $k_3 = 16$, $c_1 = 0{\cdot}1$, $c_2 = 0{\cdot}4$, $c_3 = 1{\cdot}76$, the matrix of eigenvectors is calculated as

$$\begin{bmatrix} -0{\cdot}0057 - 0{\cdot}0158\mathrm{j} & 0{\cdot}0947 + 0{\cdot}3019\mathrm{j} & 0{\cdot}4482 - 0{\cdot}0337\mathrm{j} \\ 0{\cdot}0352 + 0{\cdot}1210\mathrm{j} & -0{\cdot}0292 - 0{\cdot}0964\mathrm{j} & 0{\cdot}5271 - 0{\cdot}0396\mathrm{j} \\ -0{\cdot}0297 - 0{\cdot}1057\mathrm{j} & -0{\cdot}0503 - 0{\cdot}1574\mathrm{j} & -0{\cdot}5370 - 0{\cdot}0404\mathrm{j} \end{bmatrix}.$$

These eigenvectors look genuinely complex but they represent approximately synchronous motion. The distribution of the three eigenvectors is shown in Figure 7. They align on the complex plane approximately in-phase and

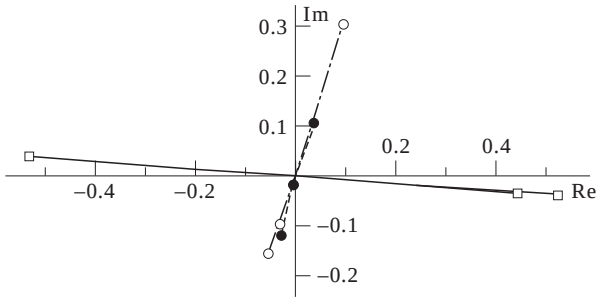

Figure 7. Distribution of the three eigenvectors of the complex plane (see example 2). For clarity, only the first three elements of each of the eigenvectors have been plotted; velocities lead the corresponding displacements (the shown quantities) approximately by a phase $\pi/2$ and are omitted. Note that the modes are nearly synchronous. Key: ●, mode 1; ○, mode 2; □, mode 3.

out-of-phase. This can also be demonstrated algebraically by rescaling the eigenvectors suitably since scaling a complex vector (using a complex scaling factor) is equivalent to scaling of magnitude as well as rotating the phasor diagram.

When the damping coefficient c_3 is changed slightly to 1·6 from 1·76, the motion is truly synchronous (the damping matrix is proportional to the stiffness matrix in this case) although the computed eigenvector may appear to be complex. Indeed the eigenvectors are real if they are scaled appropriately. Similar examples can be constructed when the system is gyroscopic and/or damped.

The non-proportionality index η for the numerical values chosen in this example (when the damping coefficient $c_3 = 1{\cdot}76$), is calculated as $\{0{\cdot}0077,\ 0{\cdot}00344,\ 0{\cdot}000005\}$ for the three modes. Since all the three indices are very small compared to unity, it may be concluded that the modes are nearly synchronous. For the case of proportional damping (when $c_3 = 1{\cdot}6$) all the three non-proportionality indices are calculated as zero as expected. In comparison, for the data of Example 1, the non-proportionality indices are given by $\{0{\cdot}0198,\ 0{\cdot}1714,\ 0{\cdot}2354,\ 0{\cdot}2381,\ 0{\cdot}2076,\ 0{\cdot}0699\}$ for the six complex modes. In the context of the discussions of Example 1, one observed that the first and the sixth damped modes are least non-proportional (hence most synchronous), since the optimally synchronous modes closely resemble the undamped natural modes. This is confirmed through the values of non-proportionality indices calculated.

5.2. AN AREA BASED NON-PROPORTIONALITY INDEX

This index of non-proportionality is inspired by the one defined in reference [9]. It is based on area of right triangles of the kind shown in Figure 2 whose orthogonal sides are p^i and h^i long. It may be noted that these triangles shrink to a straight line and correspondingly the total area becomes zero when damping becomes classical. Hence one defines a non-proportionality index for a particular mode in question in terms of these areas as

$$\rho = \sum_{r=1}^{n} A^r / A_{max}. \tag{12}$$

Where A_{max} is given by

$$A_{max} = (1/4) \sum_{r=1}^{n} l_r^2,$$

where l_r is the magnitude of the rth component of the eigenvector in question. A_{max} defined here represents the maximum possible area that a right-angled triangle can have whose hypotenuse is of length l_r.

An index of non-proportionality proposed by this author in another paper [12] is given in terms of elements of the off-diagonal entries of the modal damping matrix. In contrast, the present definition is in terms of eigenvectors. It is believed that the indices presented in this paper are more useful in assessing non-proportionality from experimental data since, in this case, information about

the system is more readily available in terms of eigenevectors as compared to the information regarding system matrices. The non-proportionality index of reference [12] on the other hand is more suitable for analytical and computational purposes.

5.3. PROPERTIES OF THE NON-PROPORTIONALITY INDICES η AND ρ

Properties commonly shared by the two indices of non-proportionality, namely, η and ρ are enumerated next.

Property 1: the non-proportionality indices lie in the range 0 to 1 i.e., $0 \leqslant \eta \leqslant 1$ and $0 \leqslant \rho \leqslant 1$.

Property 2: if synchronous motion exists (i.e., if the system is classically damped or gyroscopic coupling can be removed using the same transform as the one which uncouples inertia and stiffness terms), then indices of non-proportionality presented in this paper are equal to zero.

Property 3: if the non-proportionality indices are equal to zero, synchronous motion exists.

Property 4: for a given system, values of the non-proportionality indices are unique (but different for different mode in general).

Property 5: values of the non-proportionality indices are invariant under scaling of the eigenvectors (the scaling factor can be a complex number, in general).

Property 6: values of non-proportionality indices are continuous functions of continuous changes in the system parameters.

Property 7: if the system parameters are changed in such a manner that the phases between one phasor and all the rest increase (decrease) but the relative phases of the remaining phasors stay unchanged, then values of the non-proportionality indices increase (decrease). All the phases involved are assumed to be less than $\pi/2$.

It is clear that the non-proportionality index of reference [9] based on the modal polygons satisfies only properties 1 and 2. For the sake of brevity the formal proofs of properties 1 through to 5 are emitted, since they are taken up in the earlier discussions. Property 6 is easy to establish using the facts that (a) eigenvectors (using a scaling consistently) are continuous functions of changes in the elements of the matrices involved, and (b) the index of non-proportionality defined here is a continuous function of the elements of the eigenvectors.

Property 7 is less obvious but can be easily proved by using the fact that a sine is a monotonically increasing function whereas a cosine is a monotonically decreasing function in the range 0 to $\pi/2$. The statement of property 7 must be revised if the phases between the phasor whose sensitivity on the non-proportionality indices is being studied makes angles in the range $\pi/2$ to π with the rest of the phasors.

6. CONCLUSIONS

When classical normal modes do not exist, it is not possible to think in terms of a deformed shape in damped free motion as a mode shape. The problem of obtaining deformed configurations of the motion in these situations was

addressed. Optimally synchronous modes were defined for the case of systems that do not possess classical normal modes. The approach is based on the maximal projection of the components of an eigenvector on a radial line. Numerical examples were taken and it was observed that the optimal modes closely resemble the shape of corresponding undamped modes when damping is light. Two measures of non-proportionality indices were discussed. Certain ambiguities and inconsistencies in the definition of a non-proportionality index available in the literature were discussed.

ACKNOWLEDGMENTS

The author would like to thank Professor D. E. Newland, Department of Engineering, University of Cambridge for very useful discussions.

REFERENCES

1. L. Meirovitch *Computational Methods in Structural Dynamics*. Sijthoff & Noordhoff, 1980.
2. D. E. Newland 1989 *Mechanical Vibration*: *Analysis and Computation*. Longman.
3. K. A. Foss 1958 *Journal of Applied Mechanics* **25**, 361–364. Coordinates which uncouple the equations of motion of damped linear dynamic system.
4. T. K. Caughey 1960 *Journal of Applied Mechanics* **27**, 269–271. Classical normal modes in damped linear dynamic systems.
5. T. K. Caughey and M. E. J. O'Kelley 1965 *Journal of Applied Mechanics* **32**, 583–588. Classical normal modes in damped linear dynamic systems.
6. M. Liu and J. M. Wilson 1992 *American Institute of Aeronautics and Astronautics Journal* **30**, 2989–2991. Criterion of decoupling dynamic equations of motion of linear groscopic systems.
7. D. Z. Luo 1989 *Journal of Sound and Vibration* **135**, 351–356. A graphic explanation of undamped and damped mode shapes and its application.
8. D. E. Newland 1984 *Engineering Structures* **6**, 307–314. Calculation of the effect of resilient seating on the vibration characteristics of slender structures.
9. G. Prater and R. Singh 1986 *Journal of Sound and Vibration* **104**, 109–125. Quantification of the extent of non-proportional viscous damping in discrete vibratory systems.
10. S. S. Nair and R. Singh 1986 *Journal of Sound and Vibration* **104**, 348–350. Examination of the validity of proportional damping approximation with two further numerical indices.
11. J. Bellos and D. J. Inman 1990 *Transactions of the American Society of Mechanical Engineers*, *Journal of Vibration and Acoustics* **112**, 194–201. Frequency response of non-classically damped systems.
12. A. Bhaskar 1995 *Journal of Sound and Vibration* **184**, 59–72. Estimate of errors in the frequency response of non-classically damped systems.
13. A. Bhaskar 1990 *Dissertation submitted to Trinity College Cambridge for the Annual Fellowship Competition*. Some studies on damped vibration of linear systems.
14. I. W. Park, J. S. Kim and F. Ma 1992 *Mechanics Research Communications*, **19**, 407–413. On the modal coupling in non-clasically damped linear systems.
15. I. W. Park, J. S. Kim and F. Ma, March 1994 *Journal of Applied Mechanics* **61**, 77–83. Characteristics of modal coupling in nonclassically damped systems under harmonic excitation.